

Modeling and numerical simulation of fully Eulerian fluid-structure interaction using cut finite elements

Stefan Frei ^{*}, Tobias Knoke, Marc C. Steinbach,
Anne-Kathrin Wenske, Thomas Wick [†]

February 2, 2024

We present a monolithic finite element formulation for (nonlinear) fluid-structure interaction in Eulerian coordinates. For the discretization we employ an unfitted finite element method based on inf-sup stable finite elements. So-called ghost penalty terms are used to guarantee the robustness of the approach independently of the way the interface cuts the finite element mesh. The resulting system is solved in a monolithic fashion using Newton's method. Our developments are tested on a numerical example with fixed interface.

1 Introduction

In this work, we investigate a cut finite element discretization for fully Eulerian fluid-structure interaction (FSI). In contrast to an *Arbitrary Lagrangian Eulerian* (ALE) approach [10, 19], the benefit of a fully Eulerian formulation for FSI lies in its ability to handle (very) large deformations, topology changes, and contact problems in a straightforward way, see e.g. [15, 14, 18, 5].

The fully Eulerian approach for fluid-structure interaction has been introduced in [11, 9] and has since then been investigated and improved in several studies, such as [24, 26, 29, 23, 20, 27, 22]. The idea is to formulate both the flow and the solid problem in Eulerian coordinates in time-dependent domains $\Omega_f(t)$ resp. $\Omega_s(t)$. An accurate numerical method requires the resolution of the interface $\Gamma(t)$ separating $\Omega_f(t)$ and $\Omega_s(t)$, which can move freely depending on the solid displacements. The construction of a fitted finite

^{*}Stefan Frei, Department of Mathematics & Statistics, University of Konstanz, stefan.frei@uni-konstanz.de

[†]Tobias Knoke, Marc C. Steinbach, Anne-Kathrin Wenske, Thomas Wick, Leibniz University Hannover, Institute of Applied Mathematics {knoke,mcs,wenske,thomas.wick}@ifam.uni-hannover.de

element method is cumbersome when the interface moves, see e.g. [13, 12]. An elegant alternative is given by the cut finite element method [16, 17, 4] which is based on a fixed finite element mesh for all times. To our knowledge, this approach has not been used before in the context of fully Eulerian fluid-structure interaction. The present work is thus a first step towards such an unfitted fully Eulerian FSI formulation. As a starting point we concentrate on fixed interfaces (meaning infinitesimal displacements) in this work.

In cut finite element methods (CutFEM) [4], interface conditions are imposed by means of Nitsche’s method [21], see also [16, 17]. Moreover, additional stabilization via ghost penalty terms at the faces of cut cells is proposed, since the condition number of the system matrix suffers from cells cut into vastly different sizes, see also [3, 7]. This adaptation of Nitsche’s method is used in [6], where linear Stokes flow is coupled to a linear elastic structure through separate overlapping meshes, where the solid is described in Lagrangian coordinates on a fitted mesh and glued to the (unfitted) fluid mesh. Fictitious domain methods using cut elements with stabilized Nitsche’s method for Stokes’ problem were investigated in [8].

In this work, we employ a cut finite element method for realizing a variational-monolithic fully Eulerian fluid-structure interaction formulation on a fixed single mesh. This is specifically in extension to [6] and [8] from the ghost penalty viewpoint and all previously mentioned fully Eulerian fluid-structure interaction references. We propose a new weight function to balance the ghost penalty terms with respect to the cuts. Taylor-Hood elements are employed for the spatial discretization and a backward Euler scheme for temporal discretization. The resulting discrete monolithic formulation is treated all-at-once in the linear and nonlinear solvers.

The outline of this paper is as follows. In Section 2 our fully Eulerian fluid-structure interaction formulation is presented. Then, in Section 3, the cut finite element discretization and ghost penalty terms are introduced and described in detail. Finally, in Section 4, numerical simulations are carried out, including numerical convergence studies and a comparison to computations using the ALE method.

2 Fluid-structure interaction system

2.1 Strong form

Let $\Omega \subset \mathbb{R}^d$ be a bounded domain with $d = 2$, which is partitioned into a (fixed) fluid subdomain Ω_f and a (fixed) solid subdomain Ω_s such that $\bar{\Omega} = \bar{\Omega}_f \cup \bar{\Omega}_s$ with $\Omega_f \cap \Omega_s = \emptyset$. We assume that both Ω_f and Ω_s are parameterized by a $C^{1,1}$ boundary, such that all terms arising in the following equations are well-defined. Next, let $\Gamma_i := \bar{\Omega}_f \cap \bar{\Omega}_s$ be the interface between the subdomains, and $\Gamma_f^D \subset \Gamma_f := \partial\Omega_f \cap \partial\Omega$ and $\Gamma_s^D \subset \Gamma_s := \partial\Omega_s \cap \partial\Omega$. For the fluid velocity $v_f: \bar{\Omega}_f \times [0, T] \rightarrow \mathbb{R}^d$, the pressure $p: \bar{\Omega}_f \times [0, T] \rightarrow \mathbb{R}$, the solid velocity $v_s: \bar{\Omega}_s \times [0, T] \rightarrow \mathbb{R}^d$ and the displacement $u: \bar{\Omega}_s \times [0, T] \rightarrow \mathbb{R}^d$, we define stresses $\sigma_f := \sigma_f(v_f, p) := \rho_f \nu_f (\nabla v_f + \nabla v_f^\top) - pI$ and $\sigma_s := 2\mu_s E_s + \lambda_s \text{tr}(E_s)I$, where $E_s := \frac{1}{2}(\nabla u + \nabla u^\top + \nabla u^\top \cdot \nabla u)$ denotes the nonlinear Green-Lagrange strain, μ_s and

λ_s are the Lamé parameters, ρ_f and ρ_s are the densities of the fluid and the solid, and ν_f is the fluid viscosity. Moreover, $f: \Omega \times [0, T] \rightarrow \mathbb{R}^d$ is a given right-hand side function, $v_f^D: \Gamma_f^D \times [0, T] \rightarrow \mathbb{R}^d$ and $u^D: \Gamma_s^D \times [0, T] \rightarrow \mathbb{R}^d$ are functions on the Dirichlet boundaries, and $v_f^0: \Omega_f \rightarrow \mathbb{R}^d$, $v_s^0: \Omega_s \rightarrow \mathbb{R}^d$ and $u^0: \Omega_s \rightarrow \mathbb{R}^d$ finally describe initial values. The fully Eulerian FSI system is then defined as follows: Find (v_f, p, v_s, u) such that

$$\begin{cases} \rho_f \partial_t v_f + \rho_f (v_f \cdot \nabla) v_f - \nabla \cdot \sigma_f &= \rho_f f & \text{in } \Omega_f \times (0, T), \\ \nabla \cdot v_f &= 0 & \text{in } \Omega_f \times (0, T), \\ v_f &= v_f^D & \text{on } \Gamma_f^D \times (0, T), \\ \rho_f \nu_f \partial_n v_f - pn &= 0 & \text{on } \Gamma_f \setminus \Gamma_f^D \times (0, T), \\ v_f &= v_f^0 & \text{in } \Omega_f \times \{0\}, \\ \rho_s \partial_t v_s + \rho_s (v_s \cdot \nabla) v_s - \nabla \cdot \sigma_s &= \rho_s f & \text{in } \Omega_s \times (0, T), \\ \partial_t u + (v_s \cdot \nabla) u - v_s &= 0 & \text{in } \Omega_s \times (0, T), \\ u &= u^D & \text{on } \Gamma_s^D \times (0, T), \\ \sigma_s \cdot n &= 0 & \text{on } \Gamma_s \setminus \Gamma_s^D \times (0, T), \\ u &= u^0 & \text{in } \Omega_s \times \{0\}, \\ v_s &= v_s^0 & \text{in } \Omega_s \times \{0\}, \\ v_f &= v_s & \text{on } \Gamma_i \times (0, T), \\ \sigma_f \cdot n &= \sigma_s \cdot n & \text{on } \Gamma_i \times (0, T). \end{cases}$$

2.2 Weak formulation

Let $\mathcal{V}_f := H_0^1(\Omega_f; \Gamma_f^D)$, $\mathcal{V}_s := H^1(\Omega_s)$, $\mathcal{U} := H_0^1(\Omega_s; \Gamma_s^D)$ and $\mathcal{P} := L^2(\Omega_f)$ be given function spaces. Here, \mathcal{P} is sufficient for a unique pressure due to the outflow condition on $\Gamma_f \setminus \Gamma_f^D$. The product space is defined as $\mathcal{X} := \mathcal{V}_f \times \mathcal{V}_s \times \mathcal{U} \times \mathcal{P}$.

Problem 1 Find $v_f \in v_f^D + \mathcal{V}_f$, $p \in \mathcal{P}$, $v_s \in \mathcal{V}_s$ and $u \in u^D + \mathcal{U}$ such that $v_f = v_s$ on Γ_i and for all $(\phi_f, \psi, \phi_s, \xi) \in \mathcal{X}$:

$$\begin{aligned} & \rho_f (\partial_t v_f, \phi_f)_{\Omega_f} + \rho_f (v_f \cdot \nabla v_f, \phi_f)_{\Omega_f} + (\sigma_f, \nabla \phi_f)_{\Omega_f} + (\nabla \cdot v_f, \xi)_{\Omega_f} \\ & - (\rho_f \nu_f \nabla v_f^\top n_f, \phi_f)_{\Gamma_f \setminus \Gamma_f^D} + \rho_s (\partial_t v_s + v_s \cdot \nabla v_s, \phi_s)_{\Omega_s} + (\sigma_s, \nabla \phi_s)_{\Omega_s} \\ & + (\partial_t u + v_s \cdot \nabla u - v_s, \psi)_{\Omega_s} - (\sigma_f \cdot n_s, \phi_f - \phi_s)_{\Gamma_i} = \rho_f (f, \phi_f)_{\Omega_f} + \rho_s (f, \phi_s)_{\Omega_s}. \end{aligned}$$

2.3 Discretization and ghost penalties

To discretize in time we apply the backward Euler method. For spatial discretization we use continuous quadratic elements for the fluid velocity and continuous linear elements for the remaining solution components. Let \mathcal{T}_h be a quasi-uniform triangulation of Ω that is fitted to the boundary of the domain Ω but not to the interface Γ_i , where Γ_i is described by a level set function. Moreover, let

$$\mathcal{T}_h^f := \{T \in \mathcal{T}_h: T \cap \Omega_f \neq \emptyset\} \quad \text{and} \quad \mathcal{T}_h^s := \{T \in \mathcal{T}_h: T \cap \Omega_s \neq \emptyset\}$$

be overlapping sub-triangulations. We use the following finite element spaces on \mathcal{T}_h^i :

$$V_{h,i}^{(r)} := \{\phi \in C(\overline{\Omega_h^i}) : \phi|_T \in P_r(T) \ \forall T \in \mathcal{T}_h^i\}, \quad i \in \{f, s\},$$

where Ω_h^i denotes the domain spanned by the cells $T \in \mathcal{T}_h^i$. We define $\mathcal{V}_{h,f} := V_{h,f}^{(2)} \cap H_0^1(\Omega_f; \Gamma_f^D)$, $\mathcal{V}_{h,s} := V_{h,s}^{(1)}$, $\mathcal{U}_h := V_{h,s}^{(1)} \cap H_0^1(\Omega_s; \Gamma_s^D)$, $\mathcal{P}_h := V_{h,f}^{(1)}$ and $\mathcal{X}_h := \mathcal{V}_{h,f} \times \mathcal{V}_{h,s} \times \mathcal{U}_h \times \mathcal{P}_h$.

The interface conditions are then imposed by additional terms: the Nitsche terms (4) which ensure that the interface condition $v_f = v_s$ is satisfied, a stabilization term (5) to control the pressure (see [6]), and ghost penalty terms (6),(8), described by the ghost penalty functions $g^{h,w}(\cdot, \cdot)$ around the interface zone, that extend the coercivity of the bilinear form over the interface cells and increase stability.

Problem 2 *The discrete weak formulation reads: For $n = 1, \dots, N$ find fluid velocity, pressure, solid velocity and displacement $(v_f^h, p^h, v_s^h, u^h) := (v_f^{h,n}, p^{h,n}, v_s^{h,n}, u^{h,n}) \in \{v_f^D, 0, u^D, 0\} + \mathcal{X}_h$, where $(v_f^{h,n-1}, p^{h,n-1}, v_s^{h,n-1}, u^{h,n-1})$ are the solutions of the previous time step, such that for all $(\phi_f^h, \psi^h, \phi_s^h, \xi^h) \in \mathcal{X}_h$:*

$$\rho_f(v_f^h, \phi_f^h)_{\Omega_f} + \rho_f k(v_f^h \cdot \nabla v_f^h, \phi_f^h)_{\Omega_f} + k(\sigma_f^h, \nabla \phi_f^h)_{\Omega_f} + (\nabla \cdot v_f^h, \xi^h)_{\Omega_f} \quad (1)$$

$$- k(\rho_f \nu_f (\nabla v_f^h)^\top n_f, \phi_f^h)_{\Gamma_f \setminus \Gamma_f^D} + \rho_s(v_s^h, \phi_s^h)_{\Omega_s} + k(\sigma_s^h, \nabla \phi_s^h)_{\Omega_s} \quad (2)$$

$$+ \rho_s k(v_s^h \cdot \nabla v_s^h, \phi_s^h)_{\Omega_s} + (u^h + k(v_s^h \cdot \nabla u^h - v_s^h), \psi^h)_{\Omega_s} \quad (3)$$

$$+ kh^{-1} \rho_f \nu_f \gamma_N (v_f^h - v_s^h, \phi_f^h - \phi_s^h)_{\Gamma_i} - k(\sigma_f^h \cdot n_f, \phi_f^h - \phi_s^h)_{\Gamma_i} \quad (4)$$

$$- k(v_f^h - v_s^h, \sigma_f^h(\phi_f^h, -\xi^h) \cdot n_f)_{\Gamma_i} \quad (5)$$

$$+ 2\rho_f \nu_f k g_{v_f}^h(v_f^h, \phi_f^h) + \rho_s g_{v_s}^h(v_s^h, \phi_s^h) + k g_p^h(p^h, \xi^h) + 2\mu_s k g_u^h(u^h, \phi_s^h) \quad (6)$$

$$= \rho_f k(f, \phi_f^h)_{\Omega_f} + \rho_f (v_f^{h,n-1}, \phi_f^h)_{\Omega_f} + \rho_s k(f, \phi_s^h)_{\Omega_s} + \rho_s (v_s^{h,n-1}, \phi_s^h)_{\Omega_s} \quad (7)$$

$$+ (u^{h,n-1}, \psi^h)_{\Omega_s} + g_{v_s}^{h,w}(v_s^{h,n-1}, \phi_s^h). \quad (8)$$

Here $k = t_n - t_{n-1} > 0$ is the time step size, $h > 0$ the spatial discretization parameter, namely the maximum element size, and $\gamma_N > 0$ denotes the Nitsche parameter.

As usual, we express the weak form more compactly in terms of a semi-linear form: Find $U_h^n := (v_f^{h,n}, v_s^{h,n}, u^{h,n}, p^{h,n}) \in \{v_f^D, 0, u^D, 0\} + \mathcal{X}_h$ for the time steps $n = 1, \dots, N$, such that $A(U_h^n)(\Psi) = F(\Psi)$ for all $\Psi \in \mathcal{X}_h$.

Let \mathcal{F}_G^f denote the set of element faces $F = \bar{K}_1 \cap \bar{K}_2$ of the triangulation \mathcal{T}_h^f that do not lie on the boundary $\partial\Omega$, such that at least one of the cells K_j is intersected by the interface ($K_j \cap \Gamma_i \neq \emptyset$ for $j \in \{1, 2\}$). Analogously, we define \mathcal{F}_G^s as the set of corresponding faces of the triangulation \mathcal{T}_h^s . For a cell K cut by the interface we denote by K_{in} the part of the cell inside the considered subdomain. Using the jump terms $[[u]] = u_1|_\Gamma - u_2|_\Gamma$ with $u_i = u|_{\Omega_i}$ and $g_F^i(\varphi_1, \varphi_2) := ([[\partial_n^i \varphi_1]], [[\partial_n^i \varphi_2]])_F$, the ghost penalty

functions (with parameters $\gamma_{v_f}, \gamma_p, \gamma_{v_s}, \gamma_u$) are defined as follows:

$$\begin{aligned} g_{v_f}^{h,w}(\varphi_1, \varphi_2) &:= \gamma_{v_f} \sum_{F \in \mathcal{F}_G^f} \sum_{K: F \in \bar{K}} w(\kappa_K) \left(h g_F^1(\varphi_1, \varphi_2) + \frac{h^3}{4} g_F^2(\varphi_1, \varphi_2) \right), \\ g_p^{h,w}(\varphi_1, \varphi_2) &:= \gamma_p \sum_{F \in \mathcal{F}_G^f} \sum_{K: F \in \bar{K}} w(\kappa_K) h^3 g_F^1(\varphi_1, \varphi_2), \\ g_{v_s}^{h,w}(\varphi_1, \varphi_2) &:= \gamma_{v_s} \sum_{F \in \mathcal{F}_G^s} \sum_{K: F \in \bar{K}} w(\kappa_K) h^3 g_F^1(\varphi_1, \varphi_2), \\ g_u^{h,w}(\varphi_1, \varphi_2) &:= \gamma_u \sum_{F \in \mathcal{F}_G^s} \sum_{K: F \in \bar{K}} w(\kappa_K) h g_F^1(\varphi_1, \varphi_2). \end{aligned}$$

Here we apply a novel weight function $w: [0, 1] \rightarrow [\frac{1}{2}w_{\max}^{-1}, \frac{1}{2}w_{\max}]$, $\kappa \mapsto \frac{1}{2}w_{\max}^{1-2\kappa}$, with $w_{\max} \geq 1$, which scales the ghost penalties dependent on the cell cuts by taking the portion of the inside cell part, $\kappa_K := \text{meas}(K_{\text{in}})/\text{meas}(K)$, as the argument. Thus we penalize ‘‘bad cuts’’ more severely while ‘‘good cuts’’ (where a sufficiently large portion of the cell lies inside) are penalized less severely. Moreover, the conventional ghost penalty terms are recovered as the special case where $w_{\max} = 1$, hence $w \equiv 0.5$.

3 Nonlinear solution

To employ Newton’s method, we need the derivative

$$\begin{aligned} A'(U_h^{n,j})(\delta U_h, \Psi) &= \lim_{\epsilon \rightarrow 0} \frac{1}{\epsilon} \left(A(U_h^{n,j} + \epsilon \delta U_h)(\Psi) - A(U_h^{n,j})(\Psi) \right) \\ &= \rho_f (\delta v_f^h, \phi_f^h)_{\Omega_f} + \rho_f k (\delta v_f^h \cdot \nabla v_f^{h,j} + v_f^{h,j} \cdot \nabla \delta v_f^h, \phi_f^h)_{\Omega_f} \\ &\quad + k (\sigma_f^h (\delta v_f^h, \delta p^h), \nabla \phi_f^h)_{\Omega_f} + (\nabla \cdot \delta v_f^h, \xi^h)_{\Omega_f} - k \rho_f \nu_f (\nabla \delta v_f^h \cdot n_f, \phi_f^h)_{\Gamma_f \setminus \Gamma_f^D} \\ &\quad + \rho_s (\delta v_s^h, \phi_s^h)_{\Omega_s} + \rho_s k (\delta v_s^h \cdot \nabla v_s^{h,j} + v_s^{h,j} \cdot \nabla \delta v_s^h, \phi_s^h)_{\Omega_s} \\ &\quad + k (\sigma_s^{h'}(u^{h,j})(\delta u^h), \nabla \phi_s^h)_{\Omega_s} + (\delta u^h + k(\delta v_s^h \cdot \nabla u^{h,j} + v_s^{h,j} \cdot \nabla \delta u^h - \delta v_s^h), \psi^h)_{\Omega_s} \\ &\quad + k h^{-1} \rho_f \nu_f \gamma_N (\delta v_f^h - \delta v_s^h, \phi_f^h - \phi_s^h)_{\Gamma_i} - k (\sigma_f^h (\delta v_f^h, \delta p^h) \cdot n_f, \phi_f^h - \phi_s^h)_{\Gamma_i} \\ &\quad - k (\delta v_f^h - \delta v_s^h, \sigma_f^h (\phi_f^h, -\xi^h) \cdot n_f)_{\Gamma_i} \\ &\quad + 2 \rho_f \nu_f k g_{v_f}^h (\delta v_f^h, \phi_f^h) + \rho_s g_{v_s}^h (\delta v_s^h, \phi_s^h) + k g_p^h (\delta p^h, \xi^h) + 2 \mu_s k g_u^h (\delta u^h, \phi_s^h). \end{aligned}$$

where

$$\begin{aligned} \sigma_s^{h'}(u^{h,j})(\delta u^h) &:= 2 \mu_s E'_s(u^{h,j})(\delta u^h) + \lambda_s \text{tr}(E'_s(u^{h,j})(\delta u^h)), \\ E'_s(u^{h,j})(\delta u^h) &:= \frac{1}{2} (\nabla \delta u^h + (\nabla \delta u^h)^\top + (\nabla \delta u^h)^\top \cdot \nabla u^{j,h} + (\nabla u^{j,h})^\top \cdot \nabla \delta u^h). \end{aligned}$$

With the step length $\alpha^j \in (0, 1]$ determined by a line search, Newton’s method then takes the following form: Given an initial guess $U_h^{n,0} \in \{v_f^D, 0, u^D, 0\} + \mathcal{X}_h$, such as $U_h^{n,0} := U_h^{n-1}$, find $\delta U_h \in \mathcal{X}_h$ for $j = 0, 1, 2, \dots$, such that for all $\Psi \in \mathcal{X}_h$:

$$A'(U_h^{n,j})(\delta U_h, \Psi) = -A(U_h^{n,j})(\Psi) + F(\Psi), \quad U_h^{n,j+1} = U_h^{n,j} + \alpha^j \delta U_h.$$

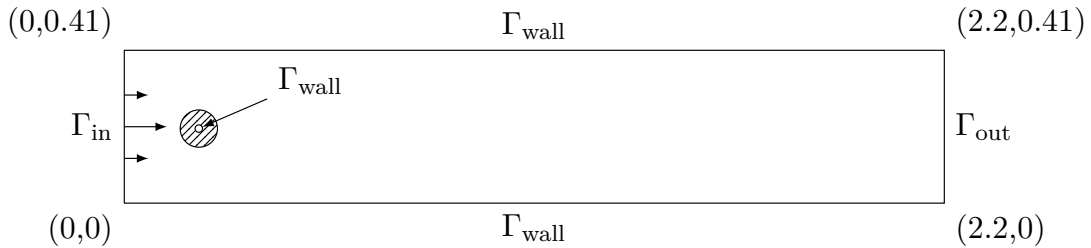


Figure 1: Configuration of laminar flow around an elastic shell with center at $(0.2, 0.2)$, inner radius of 0.01 and outer radius of 0.05 .

4 Numerical test: modified “flow around a cylinder benchmark”

In this section, we apply our numerical framework to a model problem inspired by the *flow around a cylinder benchmark* [25]. We use Newton’s method for the nonlinear solution, and therein for the linear systems the parallel sparse solver MUMPS [1]. The implementation is based on the open-source finite element library deal.II [2], in particular step 85 of the tutorial programs. Comparative computations with an arbitrary Eulerian-Lagrangian fluid-structure interaction formulation are also performed with the open-source code [30]. For our computations we neglect the convection terms $\rho_s(v_s \cdot \nabla)v_s$ and $(v_s \cdot \nabla)u$ in the structure.

In our modification of the laminar flow benchmark [25] the cylindrical hole is replaced by an elastic solid with a hole in the middle as depicted in Fig. 1. The remaining channel is filled with an incompressible Newtonian fluid. At the boundary Γ_{in} , we impose a parabolic inflow profile given by

$$v_f(0, y) = 1.5\bar{U}(4y(0.41 - y))/0.41^2$$

with mean velocity $\bar{U} = 0.2 \text{ ms}^{-1}$. At Γ_{out} a do-nothing outflow condition is applied. The boundaries Γ_{wall} supply a no-slip-condition for the fluid and a homogenous Dirichlet condition for the solid deformation. We start the time-stepping with homogeneous initial conditions and increase the inflow gradually by setting

$$v_f(t, 0, y) = \frac{1}{2}(1 - \cos(\frac{t\pi}{2}))v_f(0, y) \quad \text{for } t < 2.$$

The material parameters are based on the FSI-1 benchmark [28]: fluid density $\rho_f = 1000 \text{ kg/m}^3$, fluid viscosity $\nu_f = 0.001 \text{ m}^2/\text{s}$, solid density $\rho_s = 1000 \text{ kg/m}^3$, Lamé coefficients 0.5×10^6 and 2.0×10^6 .

The mesh consists of rectangular elements with shape regular cells except for the area of the circular solid domain Ω_s and a small neighborhood thereof.

We simulate over the time interval $[0, T]$ with $T = 25$ using the time step size $\Delta t = 1.0$. We choose the Nitsche parameter $\gamma_N = 10$, the two weight parameters $w_{\text{max}} = 3$ and $w_{\text{max}} = 1$, and ghost penalty parameters $\gamma_{v_f} = \gamma_p = \gamma_{v_s} = \gamma_u = 10^{-3}$. For Newton’s method we use the absolute tolerance 10^{-8} .

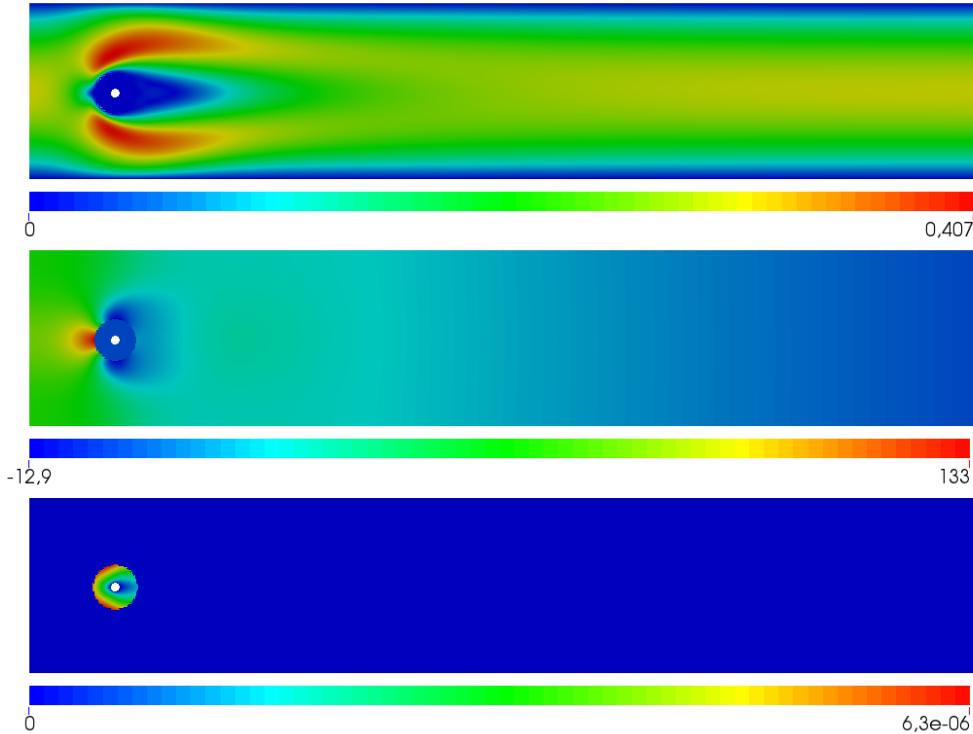


Figure 2: From top to bottom: Fluid speed $\|v_f\|_2$, pressure and displacement using the fully Eulerian approach at time $T = 25$ with $w_{\max} = 3$. As the results using the ALE approach are visually very similar to the fully Eulerian approach, we refrain from including their plots.

The interface between fluid and solid is artificially fixed to enable simple implicit time stepping. The solid material is comparatively stiff, resulting in small deformations. As quantities of interest we choose the fluid velocity at the center point of the outflow boundary, $(2.2, 0.205)$, as well as drag and lift forces around the solid. The latter are given by the line integral over the interface Γ_i , $(F_D, F_L) = \int_{\Gamma_i} \sigma_f \cdot n_f$, where n_f is the normal vector on the interface pointing towards the fluid domain. The results are shown in Table 1 and Fig. 2.

We observe no qualitative difference between our choices of the weights. However, we note that the fluctuation of the fluid velocity in cut cells is less severe for $w_{\max} = 3$ as compared to the traditional ghost penalization.

We compare these results with a corresponding computation using an ALE approach [30]. Here, the mesh is fitted to the interface and quadratic elements are used for the structural variables, which implies that the number of degrees of freedom differs from the Eulerian approach. The ALE results are shown in Table 2.

The two approaches are in good agreement, as the above tables show. We observe convergence for $h \rightarrow 0$ in all quantities of interest. The small deviations between ALE and fully Eulerian computations can be explained by the time discretization errors, as

Table 1: Quantities of interest using the FSI-1 parameters on uniformly refined meshes. The results in the top half correspond to the weight $w_{\max} = 3$ and at the bottom to $w_{\max} = 1$. Here, L denotes the refinement level. The values in the L^2 norm are taken at time $T = 25$. The drag and lift forces as well as the fluid velocity at the outflow are averaged over the time interval.

L	# dofs	$\ \nabla v_f\ _{L^2}$	$\ p\ _{L^2}$ [$\times 10^{-8}$]	$\ \nabla u\ _{L^2}$ [$\times 10^{-5}$]	F_D	F_L	$v_f(2.2, 0.205)$ ([$\times 10^{-1}$], [$\times 10^{-4}$])
0	3740	2.4152	24.4730	1.127	8.6278	0.0323	(2.734295, -1.5671)
1	13944	2.4251	24.7050	1.059	10.3264	0.0193	(2.734141, -1.6096)
2	53972	2.4283	24.7473	1.067	10.5273	0.0209	(2.734137, -1.6148)
3	211980	2.4294	24.7572	1.081	10.5484	0.0215	(2.734135, -1.6166)
4	839900	2.4297	24.7587	1.088	10.5654	0.0215	(2.734136, -1.6170)
0	3740	2.4153	24.4752	1.127	8.6236	0.0322	(2.734302, -1.5681)
1	13944	2.4251	24.7058	1.060	10.3357	0.0192	(2.734144, -1.6097)
2	53972	2.4284	24.7487	1.067	10.5495	0.0212	(2.734133, -1.6150)
3	211980	2.4295	24.7577	1.081	10.5709	0.0215	(2.734135, -1.6167)
4	839900	2.4297	24.7589	1.088	10.5864	0.0216	(2.734136, -1.6170)

Table 2: Quantities of interest using the ALE approach as with Table 1.

L	# dofs	$\ \nabla v_f\ _{L^2}$	$\ p\ _{L^2}$ [$\times 10^{-8}$]	$\ \nabla u\ _{L^2}$ [$\times 10^{-5}$]	F_D	F_L	$v_f(2.2, 0.205)$ ([$\times 10^{-1}$], [$\times 10^{-4}$])
0	8080	2.4005	24.4431	1.064	9.6868	0.1043	(2.73447, -1.56003)
1	31360	2.4183	24.6757	1.078	10.3359	0.0323	(2.73421, -1.59833)
2	123520	2.4210	24.7056	1.081	10.4933	0.0220	(2.73418, -1.60355)
3	490240	2.4211	24.7058	1.082	10.5150	0.0205	(2.73418, -1.60389)

the time step k is fixed. To further compare the two solutions we investigate the values of fluid pressure and its speed along three vertical lines $\{(x, y): 0 \leq y \leq 0.41\}$ for $x \in \{0.15, 0.25, 2.2\}$. Figure 3 depicts these results at the final time $T = 25$. Again, we observe a generally good agreement between our solution and the ALE model.

Acknowledgement Anne-Kathrin Wenske and Marc C. Steinbach gratefully acknowledge the financial support from the Deutsche Forschungsgemeinschaft (DFG, German Research Foundation) – SFB1463 – 434502799.

References

- [1] P. R. Amestoy, I. S. Duff, J.-Y. L’Excellent, and J. Koster. A fully asynchronous multifrontal solver using distributed dynamic scheduling. *SIAM J. Matrix Anal.*

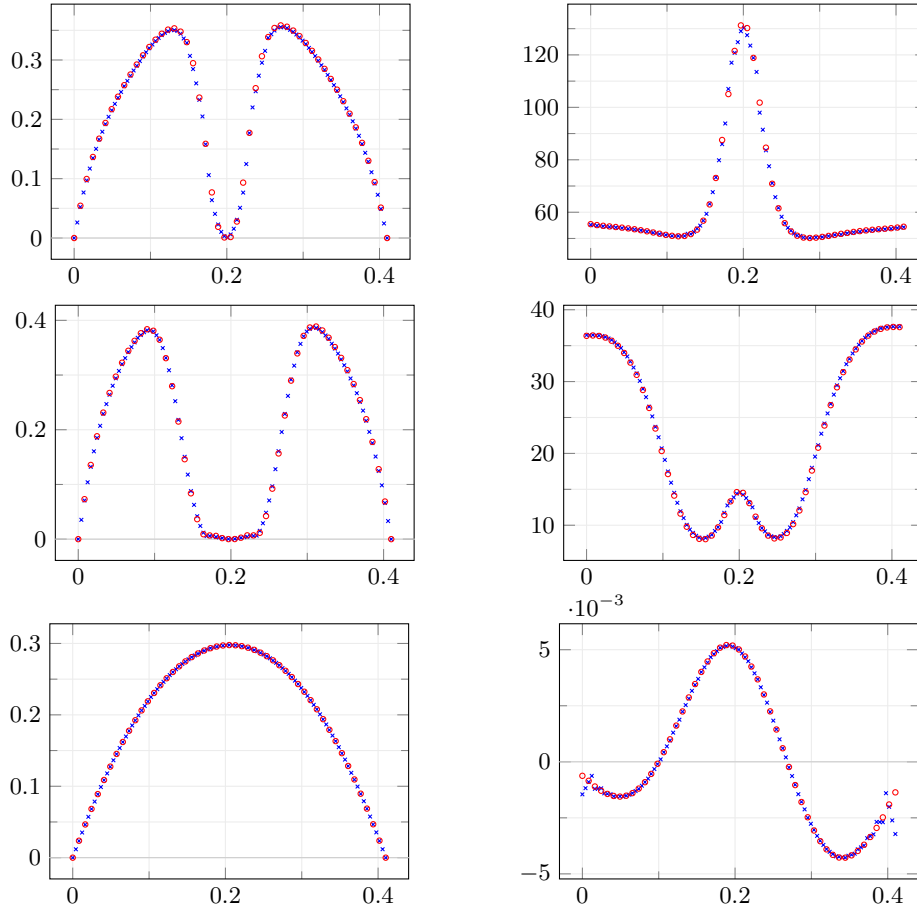


Figure 3: Profiles of fluid speed $\|v_f\|_2$ (left) and pressure (right) at time $T = 25$ with $w_{\max} = 3$ along three vertical lines: at $x = 0.15$ in front of the solid (top), at $x = 0.25$ behind the solid (middle), and at $x = 2.2$ at the outflow boundary (bottom); ALE = \times , Euler = \circ .

Appl., 23:15–41, 2001.

- [2] D. Arndt, W. Bangerth, M. Feder, M. Fehling, R. Gassmüller, T. Heister, L. Heltai, M. Kronbichler, M. Maier, P. Munch, J.-P. Pelteret, S. Sticker, B. Turcksin, and D. Wells. The `deal.II` library, version 9.4. *J. Numer. Math.*, 30(3):231–246, 2022.
- [3] E. Burman. Ghost penalty. *C.R. Math.*, 348(21):1217–1220, 2010.
- [4] E. Burman, S. Claus, P. Hansbo, M. G. Larson, and A. Massing. CutFEM: Discretizing geometry and partial differential equations. *Comp. Methods Appl. Mech. Eng.*, 104(7):472–501, 2015.
- [5] E. Burman, M. A. Fernández, and S. Frei. A Nitsche-based formulation for fluid-

- structure interactions with contact. *ESAIM. Math. Model. Numer. Anal.*, 54(2):531–564, 2020.
- [6] E. Burman and M. A. Fernández. An unfitted Nitsche method for incompressible fluid–structure interaction using overlapping meshes. *Comp. Methods Appl. Mech. Eng.*, 279:497–514, 2014.
- [7] E. Burman and P. Hansbo. Fictitious domain finite element methods using cut elements: II. A stabilized Nitsche method. *Appl. Numer. Anal. Comput. Math.*, 62(4):328–341, 2012.
- [8] E. Burman and P. Hansbo. Fictitious domain methods using cut elements: III. A stabilized Nitsche method for Stokes’ problem. *ESAIM. Math. Model. Numer. Anal.*, 48(3):859–874, 2014.
- [9] G.-H. Cottet, E. Maitre, and T. Mileent. Eulerian formulation and level set models for incompressible fluid–structure interaction. *ESAIM. Math. Model. Numer. Anal.*, 42:471–492, 2008.
- [10] J. Donea, A. Huerta, J.-P. Ponthot, and A. Rodríguez-Ferran. *Arbitrary Lagrangian–Eulerian Methods*. John Wiley & Sons, Ltd, 2004.
- [11] T. Dunne. An Eulerian approach to fluid–structure interaction and goal-oriented mesh adaption. *Int. J. Numer. Methods Fluids*, 51:1017–1039, 2006.
- [12] S. Frei. An edge-based pressure stabilization technique for finite elements on arbitrarily anisotropic meshes. *Int. J. Numer. Methods Fluids*, 89(10):407–429, 2019.
- [13] S. Frei and T. Richter. A locally modified parametric finite element method for interface problems. *SIAM J. Numer. Anal.*, 52(5):2315–2334, 2014.
- [14] S. Frei and T. Richter. An accurate Eulerian approach for fluid–structure interaction. In S. Frei, B. Holm, T. Richter, T. Wick, and H. Yang, editors, *Fluid-Structure Interaction: Modeling, Adaptive Discretization and Solvers*, Radon Series on Computational and Applied Mathematics. Walter de Gruyter, Berlin, 2017.
- [15] S. Frei, T. Richter, and T. Wick. Long-term simulation of large deformation, mechano-chemical fluid–structure interactions in ALE and fully Eulerian coordinates. *J. Comp. Phys.*, 321:874 – 891, 2016.
- [16] A. Hansbo and P. Hansbo. An unfitted finite element method, based on Nitsche’s method, for elliptic interface problems. *Comp. Methods Appl. Mech. Eng.*, 191(47):5537–5552, 2002.
- [17] P. Hansbo. Nitsche’s method for interface problems in computational mechanics. *GAMM-Mitt.*, 28(2):183–206, 2005.
- [18] F. Hecht and O. Pironneau. An energy stable monolithic Eulerian fluid–structure finite element method. *Int. J. Numer. Methods Fluids*, 85(7):430–446, 2017.

- [19] T. J. Hughes, W. K. Liu, and T. K. Zimmermann. Lagrangian-Eulerian finite element formulation for incompressible viscous flows. *Comp. Methods Appl. Mech. Eng.*, 29(3):329–349, 1981.
- [20] A. Laadhari, R. Ruiz-Baier, and A. Quarteroni. Fully Eulerian finite element approximation of a fluid-structure interaction problem in cardiac cells. *Int. J. Numer. Methods Eng.*, 96:712–738, 2013.
- [21] J. C. C. Nitsche. Über ein Variationsprinzip zur Lösung von Dirichlet-Problemen bei Verwendung von Teilräumen, die keinen Randbedingungen unterworfen sind. *Abh. Math. Semin. Univ. Hamburg*, 36:9–15, 1971.
- [22] B. Rath, X. Mao, and R. K. Jaiman. An interface preserving and residual-based adaptivity for phase-field modeling of fully Eulerian fluid-structure interaction. *J. Comput. Phys.*, 488:112188, 2023.
- [23] T. Richter. A fully Eulerian formulation for fluid–structure-interaction problems. *J. Comput. Phys.*, 233:227–240, 2013.
- [24] T. Richter and T. Wick. Finite elements for fluid–structure interaction in ALE and fully Eulerian coordinates. *Comput. Methods Appl. Mech. Engrg.*, 199(41):2633–2642, 2010.
- [25] M. Schäfer, S. Turek, F. Durst, E. Krause, and R. Rannacher. *Benchmark Computations of Laminar Flow Around a Cylinder*, pages 547–566. Vieweg+Teubner Verlag, Wiesbaden, 1996.
- [26] K. Sugiyama, S. Ii, S. Takeuchi, S. Takagi, and Y. Matsumoto. A full Eulerian finite difference approach for solving fluid-structure coupling problems. *J. Comput. Phys.*, 3(0):596–627, 2011.
- [27] P. Sun, J. Xu, and L. Zhang. Full Eulerian finite element method of a phase field model for fluid-structure interaction problem. *Comput. Fluids*, 90(0):1 – 8, 2014.
- [28] S. Turek and J. Hron. Proposal for numerical benchmarking of fluid-structure interaction between an elastic object and laminar incompressible flow. In *Fluid-Structure Interaction*, pages 371–385, Berlin, Heidelberg, 2006. Springer Berlin Heidelberg.
- [29] T. Wick. Fully Eulerian fluid-structure interaction for time-dependent problems. *Comp. Methods Appl. Mech. Eng.*, 255:14–26, 2013.
- [30] T. Wick. Solving monolithic fluid-structure interaction problems in arbitrary Lagrangian Eulerian coordinates with the deal.II library. *Arch. Num. Soft.*, 1:1–19, 2013.